

Excellence in Chemistry Research



Announcing our new flagship journal

- Gold Open Access
- Publishing charges waived
- Preprints welcome
- Edited by active scientists



Meet the Editors of ChemistryEurope





Luisa De Cola Università degli Studi di Milano Statale, Italy



Ive Hermans
University of
Wisconsin-Madison, USA



Ken Tanaka Tokyo Institute of Technology, Japan

Check for updates



www.chemeurj.org

Extended q-Range X-Ray Scattering Reveals High-Resolution Structural Details of Biomacromolecules in **Aqueous Solutions**

Jiahui Chen, [a] Olaf J. Borkiewicz, [a] Alexander V. Grishaev, *[b] Fan Zhang, [b] Mrinal K. Bera, [c] Uta Ruett, [a] and Igor Levin*[b]

Abstract: We communicate a feasibility study for highresolution structural characterization of biomacromolecules in aqueous solution from X-ray scattering experiments measured over a range of scattering vectors (q) that is approximately two orders of magnitude wider than used previously for such systems. Scattering data with such an extended qrange enables the recovery of the underlying real-space atomic pair distribution function, which facilitates structure determination. We demonstrate the potential of this method for biomacromolecules using several types of cyclodextrins (CD) as model systems. We successfully identified deviations of the tilting angles for the glycosidic units in CDs in aqueous solutions relative to their values in the crystalline forms of these molecules. Such level of structural detail is inaccessible from standard small angle scattering measurements. Our results call for further exploration of ultra-wide-angle X-ray scattering measurements for biomacromolecules.

Introduction

Our current understanding of many biological mechanisms relies on studies of biomacromolecules in their native solution states.[1] Small-angle X-ray scattering (SAXS)[2] is an important tool for structural characterization of such systems, typically applied to probe scattering vectors up to $q_{\text{max}} \approx 0.3 \text{ Å}^{-1}$, where $q = 4\pi \sin\theta/\lambda$ (θ is half the scattering angle and λ the wavelength of the incident radiation). This q_{max} value corresponds to a structural resolution $\Delta r \approx 2\pi/q_{\rm max} \approx 20 \,\text{Å}$, which is much larger than the size of basic structural units (amino acids, nucleotides, oligosaccharides, etc.) of biomacromolecules.[4] Therefore, the information extractable from typical SAXS data is mainly limited to low-resolution shapes of biomacromolecules. Obtaining finer structural details of the atomic order, for example, the primary and secondary structure of a protein,[5] ligand-binding, [6] counterion condensation, [7] etc., requires higher resolution, and, therefore, measurements to larger scattering

The structural resolution could be significantly improved by augmenting SAXS with wide-angle X-ray scattering (WAXS) to extend $q_{\text{max}}^{[8]}$ However, WAXS measurements of biomacromolecules in solutions are nontrivial as the signal is intrinsically weak and usually overwhelmed by scattering from a solvent. [9] Therefore, most WAXS studies of biomacromolecules only reach $q_{\text{max}} \approx 2 \text{ Å}^{-1}$. Furthermore, modeling WAXS data for such systems is computationally intensive, [10] often rendering structure determination and refinements impractical. Thus far, the use of WAXS has been mostly limited to the detection of ligand binding, [9] study of kinetics, [11] and verifying results of molecular dynamics (MD) simulations.[12]

Here, we explored the potential of extending the q-range of X-ray scattering measurements by two orders of magnitude for high-resolution structural characterization of biomacromolecules. We employed X-ray radiation having an energy of \approx 59 keV, which is significantly higher than the typical range from 8 keV to \approx 20 keV used for conventional SAXS/WAXS measurements. This energy enabled $q_{\text{max}} \approx 23 \text{ Å}^{-1}$ while also permitting long data-collection times required for weakly scattering biomolecular samples with negligible radiation damage. X-ray scattering data collected over such a wide qrange that provides a structural resolution $\Delta r \approx 0.3 \,\text{Å}$ are required for an accurate Fourier transform to a high-quality atomic pair distribution function (PDF). Such PDF, which reflects a histogram of all interatomic distances in the sample, [13] is not only more intuitive to interpret but also computationally less expensive to model than the reciprocal-space scattering signal. Over the last decade, PDF analyses have become a standard tool^[16] for characterizing disordered^[17] and nanostructured^[15a]

[b] Dr. A. V. Grishaev, Dr. F. Zhana, Dr. I. Levin Materials Measurement Laboratory National Institute of Standards and Technology (NIST) 100 Bureau Drive, Gaithersburg, MD, 20899 (USA) E-mail: alexander.grishaev@nist.gov igor.levin@nist.gov Homepage: https://www.ibbr.umd.edu/profiles/alexander-grishaev

https://www.nist.gov/people/igor-levin

[c] Dr. M. K. Bera NSF's ChemMatCARS University of Chicago 9700 S Cass Ave., Lemont, IL,60439 (USA)

☐ Supporting information for this article is available on the WWW under https://doi.org/10.1002/chem.202203551

[[]a] Dr. J. Chen, Dr. O. J. Borkiewicz, Dr. U. Ruett X-ray Science Division Argonne National Laboratory 9700 S Cass Ave., Lemont, IL, 60439 (USA)

Chemistry Europe

European Chemical Societies Publishing

materials. However, in typical implementations, PDF is derived from WAXS alone, with the SAXS part omitted because of instrumental limitations. The missing contribution from SAXS is usually compensated using analytical approximations, [18] but this approach is inadequate for particles having complex shapes, [19] such as those encountered for biomacromolecules. Here, we combined SAXS and WAXS signals to obtain a complete PDF that encodes structural information at multiple length scales – from sizes and shapes of biomacromolecules to fine details of their local atomic order. Theoretical background for the PDF analyses is provided in the Supporting Information. [13,14c,15]

We employed cyclodextrins (CDs)^[20] as model systems to assess the feasibility of the proposed approach. CDs are cyclic polysaccharides with α -1,4-glycosidic bonds linking α -D-glucopyranosides units. The most common types of CDs are alpha-CD (ACD), beta-CD (BCD), and gamma-CD (GCD). ACD, BCD, and GCD incorporate six, seven, and eight basic units, respectively (Figure 1a). CDs are of interest for both pharmaceutical applications and fundamental research. These molecules, which contain hydrophilic hydroxyl groups on the rims of the cones, are soluble in water. At the same time, their hydrophobic cavity can accommodate guest molecules with suitable sizes via host-guest interactions. Because of this combination of hydrophilicity and the ability to host hydrophobic guest species, CDs can increase solubility and modify properties of guest molecules, thereby helping to formulate small pharmaceutical compounds

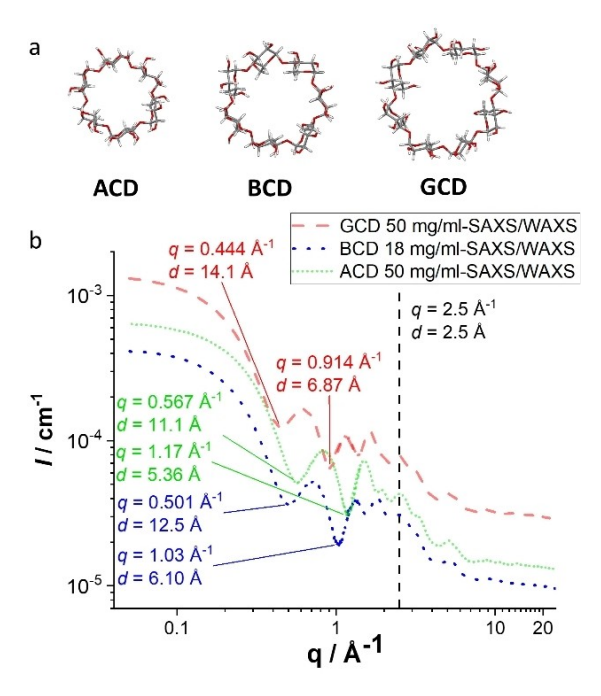


Figure 1. (a) Rendering of ACD, BCD, and GCD crystalline structures. Crystalline water molecules are omitted for clarity. (b) Log-Log plot of the scattering intensity (l) vs. scattering vector (q) for the merged SAXS and WAXS data from the CD aqueous solutions. Plots with error bars can be found in the Supporting Information. The scattering profiles were obtained by subtracting the solvent scattering, measured separately, from the total signal. Red: 50 mg/ml GCD; Blue: 18 mg/ml BCD; Green: 50 mg/ml ACD. d is the real-space distance calculated from q.

(e.g., recent examples of remdesivir^[21]) and build complex self-assembled supramolecular structures.^[22] The spatial dimensions of CDs and their elemental compositions are comparable to biomacromolecules such as small proteins or oligosaccharides. Moreover, CDs of different sizes can exhibit different ring conformations and/or flexibilities, resembling the variability of the torsion angles between individual units in biomacromolecular chains. The conformation of CDs in solutions determines host-guest interactions; ^[23] therefore, adequate understanding of structural details in these systems is key to developing their applications. Additionally, MD simulations of CDs in solutions are available, requiring experimental validation.^[24] All these factors make CDs well-suited for establishing the structure determination methodology.

Results and Discussion

The structures of ACD, BCD, and GCD determined in their crystalline states, along with their respective experimental spliced SAXS and WAXS signals are displayed in Figure 1. Some information is apparent already from visual inspection of the scattering profiles, which feature two regions separated by the vertical dashed line at 2.5 Å⁻¹. For q < 2.5 Å⁻¹, the three profiles are dominated by the SAXS form factors associated with the overall shapes of the molecules (e.g., the first two minima are related to the molecular dimensions.) For $q > 2.5 \text{ Å}^{-1}$, the slowly varying signals, albeit devoid of visually prominent features (e.g., peaks, troughs), reflect the local atomic ordering, discoverable in the PDF if this scattering is included in the Fourier transform. The high-q region appears similar for the three structures, suggesting similar rigidity of the glycosidic units, regardless of the number of glucopyranose units. We performed standard analyses^[3] of the SAXS data for solutions with different concentrations of CDs to verify data quality and the appropriateness of our data acquisition protocols. These results, along with the effects of the omitted SAXS and WAXS signals on the Fourier transform of the scattering data, are summarized in the Supporting Information.

PDFs of CDs were extracted from the scattering profiles to obtain interatomic correlations in these molecules. The blue lines in Figure 2 represent the experimental PDFs. The low-r (< 4.5 Å) peaks correspond to interatomic distances within the glycosidic units and hydrogen bonds. These peaks are relatively sharp, as expected for rigid units. The high-r features reflect the inter-glycosidic correlations and are significantly broader because of both the thermal motion of these units and the progressively increasing number of atomic pairs at longer distances, which lead to peak overlap.

Structural refinements of the CD molecules against their PDF profiles were performed to determine the behavior of glycosidic units. According to the published crystal structures, NMR data and MD simulations, [20b,24-25] the conformation of the CD macrocycle is relatively rigid due to the overall cyclic restrictions and inter-glycosidic hydrogen bonds. In crystals, glycosidic units deviate from their common mean plane by less than 0.25 Å, while the torsion angles between these units are

5213765,

3, 31, Downloaded from https://chemistry-europe.online.library.wiley.com/doi/10.1002/chem.202203531 by rgome National Laboratory, Wiley Online Library on [02/06/2023], See the Terms and Conditions (https://online.library.wiley.com/emistry-europe.online.library.wiley.com/doi/10.1002/chem.202203531 by rgome National Laboratory, Wiley Online Library on [02/06/2023], See the Terms and Conditions (https://online.library.wiley.com/emistry-europe.online.library.wiley.com/doi/10.1002/chem.202203531 by rgome National Laboratory, Wiley Online Library on [02/06/2023], See the Terms and Conditions (https://online.library.wiley.com/emistry-europe.online.library.wiley.com/emistry-europe.online.library.wiley.com/emistry-europe.online.library.wiley.com/emistry-europe.online.library.wiley.com/emistry-europe.online.library.wiley.com/emistry-europe.online.library.wiley.com/emistry-europe.online.library.wiley.com/emistry-europe.online.library.wiley.com/emistry-europe.online.library.wiley.com/emistry-europe.online.library.wiley.com/emistry-europe.online.library.wiley.com/emistry-europe.online.library.wiley.com/emistry-europe.online.library.wiley.com/emistry-europe.online.library.wiley.com/emistry-europe.online.library.wiley.com/emistry-europe.online.library.wiley.com/emistry-europe.online.library.wiley.com/emistry-europe.online.library.wiley.com/emistry-europe.online.library.wiley.com/emistry-europe.online.library.wiley.com/emistry-europe.online.library.wiley.com/emistry-europe.online.library.wiley.com/emistry-europe.online.library.wiley.com/emistry-europe.online.library.wiley.com/emistry-europe.online.library.wiley.com/emistry-europe.online.library.wiley.com/emistry-europe.online.library.wiley.com/emistry-europe.online.library.wiley.com/emistry-europe.online.library.wiley.com/emistry-europe.online.library.wiley.com/emistry-europe.online.library.wiley.com/emistry-europe.europe.europe.europe.europe.europe.europe.europe.europe.europe.europe.europe.europe.europe.europe.europe.europe.europe.europe.europe.europe.europe.europe.europe.eur

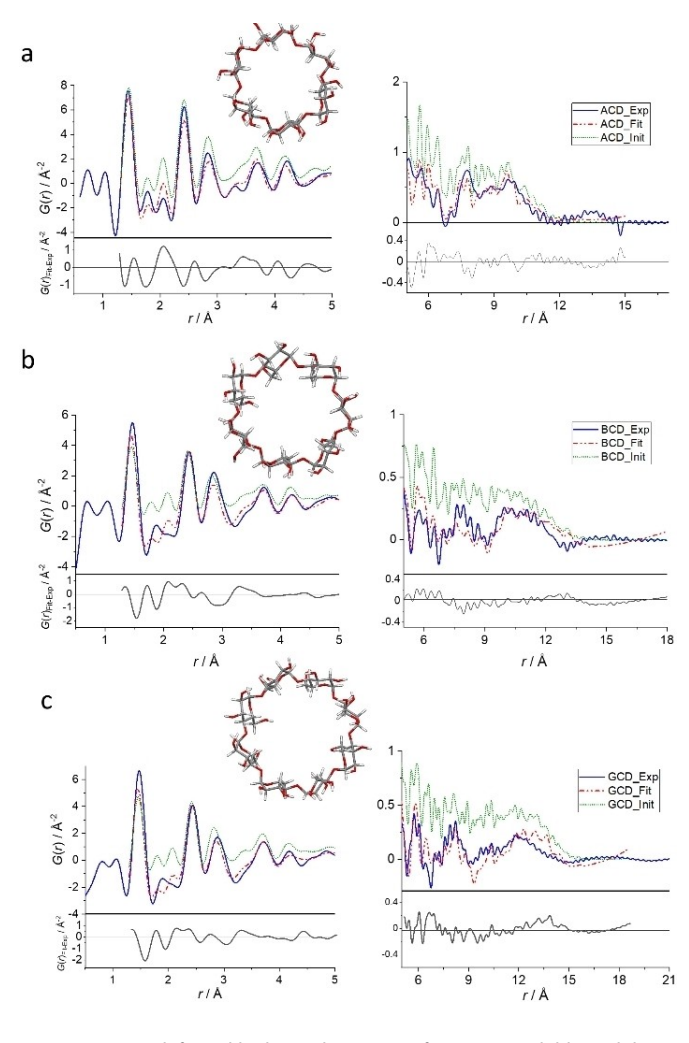


Figure 2. Low-r (left) and high-r (right) region of experimental (blue solid line), calculated from the initial structures adopted from the database (green dotted line), and fitted (red dash line) PDFs of (a) ACD, (b) BCD, and (c) GCD. Insets display the corresponding structural models with the hydration-layer water molecules omitted for clarity.

nearly constant . [20b] However, in solution, the torsion angle rotations about the glycosidic bonds can significantly affect oligosaccharide conformations.[25b] Therefore, our models allowed such motion by refining the torsion angles of glycosidic bonds. Also, CD molecules form hydrogen bonds in aqueous solutions with water both at the surface and inside the CD cavity. [23] Therefore, such water molecules were included in the structural models (more details are in the Supporting Information). The thermal motion of the water molecules was refined to recreate the contributions of the hydration layer and inner water clusters to the PDF signal.

The refined structure of ACD superimposed on the initial model from the crystal-structure database is displayed in Figure 3; similar results for BCD and GCD are listed in the Supporting Information. Figure 2 compares PDF profiles for the initial (green dots) and refined structures (red lines). The differences between the high-r portions of the two signals are significant. Asymmetric torsion angles for each glycosidic bond in ACD differed from those in the initial crystal structure by $\approx 4^{\circ}$

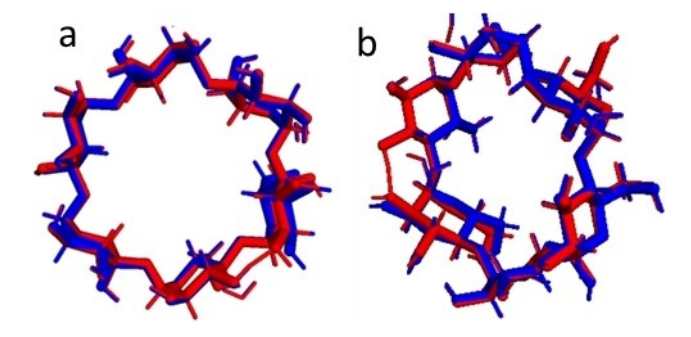


Figure 3. Refined structural model of ACD. Hydration water molecules are omitted for clarity. Superimposed refined structure (red) of ACD from the PDF analysis and the initial structure from the database (blue), (a) top and (b) 45°-tilted views of the secondary rim of ACD. The refined models for the other two types of CDs are included in the Supporting Information.

(positive for the hydroxymethyl groups rotating outwards from the CD macrocycle). For both BCD and GCD, the differences from their respective crystalline models were $\approx 3^{\circ}$. The more significant torsion angle differences in ACD relative to two other types can be attributed to different strains in the overall macrocycle conformations, [24] PDF-refined models are also markedly less symmetric than the approximately circular structures determined in their respective crystalline forms, possibly reflecting distortions of the individual oligosaccharides in solutions at 298 K.

In the case of CDs, knowledge of fine structural details, such as torsion angles within the building units, could increase understanding of host-guest interactions - as required, for example, to explain the unusually high affinity between CDs and guest boron clusters, the size of which precisely match that of the CD cavity. [26] Yet, such details would be inaccessible from typical SAXS experiments and modeling. For example, Figure 4 shows a reconstructed structure^[14a,b] from the SAXS component of the ACD data. Although this model correctly describes the approximate size of the ACD molecule, the details of its shape (e.g., six repeat units) and closing cycles are either missing or misrepresented. Possible reasons include the limited resolution and information content of the SAXS data. Even the SAXS cutoff of 1 Å^{-1} results in the structural resolution of only \approx 6 Å, which is coarser than the dimensions of a glycosidic unit. Another set of factors is the approximations and regularization biases

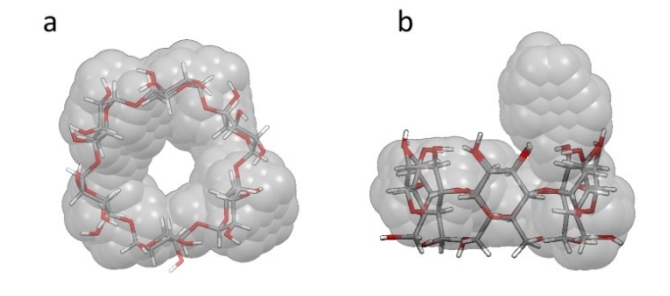


Figure 4. Reconstructed structure of ACD from SAXS ($q < 1 \text{ Å}^{-1}$) (light gray envelope) overlayed onto the model obtained from the PDF refinements (gray/red stick rendering). (a) Top view, (b) side view.

Chemistry Europe European Chemical Societies Publishing

involved in converting the SAXS intensity into a pair-density distribution function and then into a three-dimensional structural model. [14a,b] As we show here, extending the $q_{\rm max}$ limit of the scattering data to yield an adequate-quality PDF leads to much-improved resolution and scope of structural solutions.

CDs are smaller and more rigid and ordered than many biomacromolecules facilitating refinements of their structures from the PDF alone using existing crystallographic methods and software. For biomacromolecules, such as proteins or oligonucleotides, a PDF, which effectively represents an average over an ensemble of molecules in the sample, will still serve as a high-fidelity "fingerprint" of the overall molecular structure. However, finding a representative structural solution will require integrating this PDF signal with other data from methods such as NMR to constrain the model. Unlike traditional crystallographic descriptors employed here, with atomic motion parameterized using atomic displacement parameters (ADP), fully atomistic refinements of the instantaneous atomic positions encoded in the solution-scattering data and including several conformations might be possible, though it will necessitate further development of the existing algorithms and computer programs. Concurrently, PDF data can provide powerful constraints and benchmarks for MD simulations of biomacromolecules. The fast speed of real-space PDF calculations also makes PDF measurements attractive for use with high-throughput methods, including training machine-learning models.

Conclusions

We demonstrated that combining SAXS and WAXS measurements to span a q range from $\approx 0.05 \text{ Å}^{-1}$ to 23 Å⁻¹, holds promise for the unprecedented structural characterization of biomacromolecules in native solution environments and further exploration is ongoing. A principal advantage of having a scattering signal over such an ultra-wide q-range is the ability to convert it to a high-resolution atomic pair-distribution function which facilitates the determination of structural details. We used CDs as example systems to illustrate the potential of this approach. We successfully determined torsion angles for the glycosidic bonds for CDs in solutions showing them to deviate from those in the crystalline forms of these molecules. Such information is inaccessible from standard SAXS measurements. Using WAXS data measured to the conventional q_{\max} of 2 Å^{-1} to 3 Å^{-1} could possibly permit the determination of torsion angles; however, this analysis would have to be performed in reciprocal space, which is much more challenging and computationally intensive than the PDF analyses employed here. The methodology, including the data acquisition and analysis protocols established in this feasibility study, are envisioned to provide a foundation for further development of ultra-wide angle X-ray scattering measurements toward highresolution structural characterization of biomacromolecules.

Experimental Section

Materials: ACD, BCD, and GCD powders were purchased from Sigma-Aldrich and used without further purification. The sample solutions were prepared by dissolving these powders in deionized water. For ACD and GCD, sample concentrations of 12.5 mg/ml, 25 mg/ml and 50 mg/ml were used. For BCD, the concentrations were 12.5 mg/ml and 18 mg/ml, with the latter close to the solubility limit. Data collected for these solutions containing different concentrations of CDs were used to assess the reproducibility and reliability of both SAXS and WAXS measurements. All measurements were conducted at ambient temperature (298 K).

SAXS: These measurements were performed at the NSF ChemMat-CARS (15-ID-D) beamline of the Advanced Photon Source (APS) at Argonne National Laboratory. The sample solutions were placed in a 1.5 mm diameter, thin-walled quartz capillary tube flow cell, and the solutions were flown continuously to mitigate radiation damage. Data frames were collected using a Pilatus3X 300 K detector with a 1 mm Si chip and a sample-to-detector distance of 0.57 m with the X-ray energy of 20 keV or 16 keV. We performed separate measurements for the empty setup, empty flow cell, and water flowing through the flow cell to determine the background to be subtracted from the total intensity to isolate the signal from the sample molecules. The exposure time for each measurement was 2 min. The q-range of the data was from $q_{\rm min} \approx 0.05 \, {\rm \AA}^{-1}$ to $q_{\rm max}$ \approx 1.4 Å⁻¹.

X-ray total scattering: These measurements were conducted at beamline 11-ID-B of the APS. Data were recorded on a Perkin-Elmer amorphous-Si two-dimensional detector (2048 × 2048 pixels and 200×200 μm pixel size) mounted downstream from the sample perpendicular to the beam path with a sample-to-detector distance of \approx 180 mm. The X-ray energy was 58.76 keV (λ = 0.2115 Å). The sample solutions were placed in 3 mm diameter thin-walled borosilicate glass NMR tubes. The samples were oscillated during measurements along the tube axis to mitigate radiation damage. Scattering from the empty setup, empty NMR tube, and water in the NMR tube was measured separately for background subtraction. Each data frame recorded on the detector consisted of 120 subframes with an exposure time of 0.15 s per subframe. We used a 3 min "sleep time" between the data frames and discarded the first three frames to avoid potential artifacts caused by the presence of a residual signal on the detector. For the sample solutions and the empty setup, the total exposure time was 60 min. For the empty NMR tube and water in this tube, the exposure time was 120 min.

Two-dimensional images of the scattering patterns were azimuthally integrated and converted to one-dimensional intensity(I) versus q traces using GSAS II.[4] We used PDFgetX2 software[5] to correct the I(q) signal for Compton scattering and to subtract the backgrounds from the flow cell and water, converting I(q) first to S(q) and then to G(r) per Equation (5) in the Supporting Information. The q-range included in the Fourier transform was from $q_{min} = 1 \text{ Å}^{-1}$ to $q_{\text{max}} \approx 23 \text{ Å}^{-1}$.

Structural refinements: Structures of CD molecules were refined against the experimental G(r) using TOPAS.^[6] The starting models were adopted from the Cambridge Crystal Structure Database (CCDC, Table S1). These models were added a hydration layer and placed in an otherwise empty unit cell, sufficiently large to prevent contributions from interatomic distances between the molecule and its aliases created by the periodic boundary conditions imposed by the software. The glucopyranosides units were constrained as rigid, with each unit allowed to rotate around its center. The total number of rotational variables was 6 for ACD, 7 for BCD, and 8 for GCD. We used two ADP parameters to describe thermal motion - one for the atoms in the CD structure and another for the

s, 31, Downloaded from https://chemistry-europe.online/library.wiley.com/doi/10.1002/chem.202203551 by Argonne National Laboratory, Wiley Online Library on [02/06/2023]. See the Terms and Conditions (https://onlinelibrary.wiley.com/rems-

and-conditions) on Wiley Online Library for rules of use; OA articles are governed by the applicable Creative Commons License

water molecules in the hydration layer; the PDF alone did not support refinements of individual ADPs. We employed a simulated annealing algorithm implemented in TOPAS. The objective function minimized during fitting was the sum of squares of the weighted differences between the observed and calculated PDF signals at each r-value. The final refined structure corresponded to the global minimum of this objective function as identified by the software. The existing literature on CDs^[24,25] is inconclusive regarding their most probable conformational states but suggests limited conformational variability of these molecules. Our structural models assumed a single conformation for CDS because the PDF alone was insufficient for including multiple conformations. In the future, combining PDF and NMR data will help develop a more accurate model of the conformational states.

Certain commercial equipment, instruments, materials, suppliers, or software are identified in this paper to foster understanding. Such identification does not imply recommendation or endorsement by the National Institute of Standards and Technology (NIST), nor does it imply that the materials or equipment identified are necessarily the best available for the purpose.

Acknowledgements

The SAXS measurements were conducted at NSF's ChemMat-CARS, which is supported by the Divisions of Chemistry and Materials Research, National Science Foundation, under grant number NSF/CHE 1834750. The total X-ray scattering experiment was performed at 11-ID-B. Use of the Advanced Photon Source, an Office of Science User Facility operated for the U.S. Department of Energy (DOE) Office of Science by Argonne National Laboratory, was supported by the U.S. DOE under Contract No. DE-AC02-06CH11357.

Conflict of Interest

The authors declare no conflict of interest.

Data Availability Statement

The data that support the findings of this study are available from the corresponding author upon reasonable request.

Keywords: biomacromolecules · cyclodextrin · pair distribution function analysis · SAXS/WAXS · total scattering

- [1] S. Curry, Interdiscip. Sci. Rev. 2015, 40, 308-328.
- [2] T. Li, A. J. Senesi, B. Lee, Chem. Rev. 2016, 116, 11128-11180.

- [3] C. M. Jeffries, J. Ilavsky, A. Martel, S. Hinrichs, A. Meyer, J. S. Pedersen, A. V. Sokolova, D. I. Svergun, Nat. Rev. Methods Primers 2021, 1, 70.
- [4] S. R. K. Ainavarapu, J. Brujić, H. H. Huang, A. P. Wiita, H. Lu, L. Li, K. A. Walther, M. Carrion-Vazquez, H. Li, J. M. Fernandez, Biophys. J. 2007, 92, 225-233.
- [5] T. Phan-Xuan, E. Bogdanova, A. Millqvist Fureby, J. Fransson, A. E. Terry, V. Kocherbitov, Mol. Pharm. 2020, 17, 3246-3258.
- [6] David D. L. Minh, L. Makowski, Biophys. J. 2013, 104, 873-883.
- [7] S. A. Pabit, A. M. Katz, I. S. Tolokh, A. Drozdetski, N. Baker, A. V. Onufriev, L. Pollack, J. Chem. Phys. 2016, 144, 205102.
- [8] a) L. Makowski, D. J. Rodi, S. Mandava, S. Devarapalli, R. F. Fischetti, J. Mol. Biol. 2008, 383, 731-744; b) M. Cammarata, M. Levantino, F. Schotte, P. A. Anfinrud, F. Ewald, J. Choi, A. Cupane, M. Wulff, H. Ihee, Nat. Methods 2008, 5, 881-886.
- [9] L. Makowski, J. Struct. Funct. Genomics 2010, 11, 9-19.
- [10] C. J. Knight, J. S. Hub, Nucleic Acids Res. 2015, 43, W225-W230.
- [11] H. S. Cho, F. Schotte, V. Stadnytskyi, A. DiChiara, R. Henning, P. Anfinrud, J. Phys. Chem. B 2018, 122, 11488-11496.
- [12] M. Bin, R. Yousif, S. Berkowicz, S. Das, D. Schlesinger, F. Perakis, Phys. Chem. Chem. Phys. 2021, 23, 18308-18313.
- [13] E. Takeshi, S. J. L. Billinge, in Pergamon Materials Series, Vol. 16 (Eds.: T. Egami, S. J. L. Billinge), Pergamon, 2012, pp. 55-111.
- [14] a) D. I. Svergun, A. V. Semenyuk, L. A. Feigin, Acta Crystallogr. Sect. A 1988, 44, 244–251; b) D. I. Svergun, J. Appl. Crystallogr. 1991, 24, 485– 492; c) K. Manalastas-Cantos, P. V. Konarev, N. R. Hajizadeh, A. G. Kikhney, M. V. Petoukhov, D. S. Molodenskiy, A. Panjkovich, H. D. T. Mertens, A. Gruzinov, C. Borges, C. M. Jeffries, D. I. Svergun, D. Franke, J. Appl. Crystallogr. 2021, 54, 343-355.
- [15] a) A. Gagin, A. J. Allen, I. Levin, J. Appl. Crystallogr. 2014, 47, 619-629; b) C. J. Benmore, O. L. G. Alderman, D. Robinson, G. Jennings, A. Tamalonis, J. Ilavsky, E. Clark, E. Soignard, J. L. Yarger, J. K. R. Weber, Nucl. Instrum. Methods. Phys. Res. A 2020, 955, 163318; c) B. H. Toby, R. B. Von Dreele, J. Appl. Crystallogr. 2013, 46, 544-549; d) A. A. Coelho, J. Appl. Crystallogr. 2018, 51, 210-218; e) L. B. Skinner, C. Huang, D. Schlesinger, L. G. M. Pettersson, A. Nilsson, C. J. Benmore, J. Chem. Phys. 2013, 138, 074506; f) X. Qiu, J. W. Thompson, S. J. L. Billinge, J. Appl. Crystallogr. 2004, 37, 678-678.
- [16] M. W. Terban, S. J. L. Billinge, Chem. Rev. 2022, 122, 1208–1272.
- [17] T. Dykhne, R. Taylor, A. Florence, S. J. L. Billinge, Pharm. Res. 2011, 28, 1041-1048.
- [18] D. Olds, H.-W. Wang, K. Page, J. Appl. Crystallogr. 2015, 48, 1651–1659.
- [19] T.-M. Usher, D. Olds, J. Liu, K. Page, Acta Crystallogr. Sect. A 2018, 74, 322-331.
- [20] a) G. Crini, Chem. Rev. 2014, 114, 10940-10975; b) W. Saenger, J. Jacob, K. Gessler, T. Steiner, D. Hoffmann, H. Sanbe, K. Koizumi, S. M. Smith, T. Takaha, Chem. Rev. 1998, 98, 1787-1802.
- [21] a) L. Szente, I. Puskás, T. Sohajda, E. Varga, P. Vass, Z. K. Nagy, A. Farkas, B. Várnai, S. Béni, E. Hazai, Carbohydr. Polym. 2021, 264, 118011; b) Vol. 2022.
- [22] Z. Liu, Y. Liu, Chem. Soc. Rev. 2022, 51, 4786-4827.
- [23] A. A. Sandilya, U. Natarajan, M. H. Priya, ACS Omega 2020, 5, 25655-25667.
- [24] J. Gebhardt, C. Kleist, S. Jakobtorweihen, N. Hansen, J. Phys. Chem. B 2018, 122, 1608-1626.
- [25] a) H. Dodziuk, J. Mol. Struct. 2002, 614, 33-45; b) K. J. Naidoo, M. R. Gamieldien, J. Y.-J. Chen, G. Widmalm, A. Maliniak, J. Phys. Chem. B 2008. 112. 15151-15157.
- [26] a) K. I. Assaf, M. S. Ural, F. Pan, T. Georgiev, S. Simova, K. Rissanen, D. Gabel, W. M. Nau, Angew. Chem. Int. Ed. 2015, 54, 6852-6856; Angew. Chem. 2015, 127, 6956-6960; b) J. Chen, J. Luo, S. Bekele, M. Tsige, T. Liu, ChemPlusChem 2020, 85, 2316-2319.

Manuscript received: November 15, 2022 Accepted manuscript online: January 16, 2023 Version of record online: April 21, 2023